



www.ericjournal.ait.ac.th

Application of Green Roof Landscape Design Incorporating Building Energy Efficiency Concepts and Analysis of Urban Thermal Efficiency Benefits

Ruoxu Guo^{*,1} and Sa Zhao*

ARTICLE INFO

Article history:

Received 31 March 2025

Received in revised form

22 July 2025

Accepted 30 July 2025

Keywords:

Benefit analysis

Concept of building energy efficiency

Green roof

Landscape design

Urban thermal efficiency

ABSTRACT

Green roof gardens, as an emerging urban greening method, have potential benefits in alleviating urban heat island effect and reducing building energy consumption. To evaluate the actual benefits of green roof garden design in reducing building energy consumption, carbon emissions, and extending the service life of building surface materials, a carbon balance-based carbon balance accounting model for roof gardens is constructed. The analytic hierarchy process-entropy weight method is used to weight analyze the evaluation index system of green roof gardens, and the performance differences between green roofs and common building roofs are compared and studied. The research results find that the annual energy consumption of green roofs is 180 kWh/m², which is significantly lower than the 490 kWh/m² of common building roofs. The carbon emissions are 3 tons, which is lower than 5 tons for common building roofs. After 30 months, the aging degree of green roof materials is 39%, much lower than the 78% of common building roofs. Green roof garden design has significant advantages in energy conservation and emission reduction, as well as extending the service life of materials, and contributes significantly to advancing sustainable urban growth. The research provides scientific basis for urban planners and architects in green building project decision-making, promoting innovation and application of green building technology.

1. INTRODUCTION

The intensification of urban expansion has resulted in various environmental challenges, especially the enhancement of urban heat island effect and the increase in building energy consumption, which pose severe challenges to the sustainable development of cities. Green roof garden design, as an innovative urban greening technology, has received widespread attention due to its potential benefits in reducing building surface temperature, decreasing energy consumption, and improving urban ecological environment [1], [2]. Although the ecological and environmental benefits of green roof garden design have been confirmed by multiple studies, the comprehensive evaluation of its benefits in building energy efficiency and urban thermal efficiency is still insufficient, especially the quantitative analysis of performance differences under different climatic conditions and the impact on the aging of building surface materials. In addition, the promotion of green roof garden design is constrained by spatial limitations and water resource management, which limit its widespread application worldwide. Therefore, there exists a pressing necessity for the adoption of a systematic methodology to assess the genuine

advantages of green roofs concerning building energy efficiency and urban thermal performance, as well as to investigate their influence on the degradation of building surface materials. This endeavor is crucial for effectively guiding the planning, design, and policy formulation of green roof gardens [3], [4].

To transcend the constraints inherent in conventional green roof renovation practices, an innovative concept has been introduced, with the dual objectives of mitigating global climate change and fostering urban cooling via the ecological metamorphosis of urban infrastructure. Jamei *et al.* used the ENVI met tool to evaluate the air temperature and thermal comfort of the roof and pedestrian area of the National Treasury Square and quantified the cooling effect of complex green roofs. The data showed that installing green roofs notably decreased the roof-level temperature by 1.5°C and increased the thermal comfort by 2.38°C during the scorching summer heat [5]. Although the importance of urban greening is self-evident, the constraints of space and water resources limit its global popularity. Rabbani *et al.* investigated the water consumption of bamboo and calamus under different soil amendments and humic acid treatments. The research found that combining bentonite and cordierite soil matrix could construct a sustainable green roof system by optimizing coverage, water conservation, and enhancing aesthetics [6]. Liu *et al.* optimized the design of sponge city facilities in response to the impermeable characteristics of the Changzhen Depot of the Shenzhen Metro. The research showed that under the

<https://doi.org/10.64289/iej.25.0309.4933650>

*Xuchang Vocational Technical College, Xuchang 461000, China.

¹Corresponding author;

E-mail: g25524646@126.com

www.ericjournal.ait.ac.th

target of 70% annual runoff control rate, optimized sponge city facilities could meet the design goal of zero runoff. These facilities could effectively reduce the runoff, peak flow, and flow coefficient of the Changzhen vehicle depot [7]. Akar explored the potential of using three different substrates, coconut meat, loofah web, and perlite, to design succulent plant green roofs to enhance their effectiveness. The study divided the plant growth medium in the planting layer into four different groups: soil-coconut oil, soil-loofah, soil-perlite, and pure soil. The outcomes indicated that perlite performed better than other options in most evaluation variables [8]. In response to the coexistence of the scarcity of urban green Spaces and the rising energy consumption of buildings, Gohari *et al.* proposed incorporating green roofs into the energy-saving renovations of residential and public buildings, and comprehensively considering thirteen sub-indicators in the three dimensions of environment, economy and society. The research showed that roof lifespan and air quality were the top priorities for the two types of buildings. It was confirmed that green roofs had significant benefits in extending the service life of roofing materials, reducing energy consumption and improving urban thermal efficiency, providing a replicable path for roof garden design that integrates energy-saving concepts in dry and hot areas [9]. In response to the problems of slow promotion of green roofs and the lack of quantitative comparison of energy-saving effects in developing countries, Durdyev *et al.* proposed the "government-knowledge-policy" three-dimensional eighteen strategies and integrated expert opinions using the fuzzy Analytic Hierarchy Process (AHP). The results showed that roof lifespan and air quality had the highest weight in residential and government buildings. It was confirmed that green roofs could simultaneously enhance building energy conservation and urban thermal efficiency [10].

In summary, research has confirmed the positive effects of green roofs in reducing building surface temperature, decreasing energy consumption, improving urban microclimate, and enhancing urban biodiversity. However, most studies focus on the short-term benefits analysis of green roofs, with relatively less research on long-term performance and sustainability. In addition,

the promotion and application of green roofs are constrained by spatial limitations and water resource management, which limit their widespread use worldwide. The research aims to take the concept of building energy conservation as the core and systematically evaluate the comprehensive benefits of green roof garden design in reducing building energy consumption, lowering carbon emissions (CEs), and delaying the aging of building surface materials. The research aims to construct a carbon balance accounting model for rooftop gardens based on carbon balance, quantify the CEs and plant carbon absorption processes of green rooftops throughout their entire life cycle, and clarify their potential contributions to achieving carbon neutrality at the urban level. Meanwhile, the AHP - entropy weight method is introduced to construct the evaluation index system of green roof gardens. By taking into thorough account a multitude of factors—including spatial planning, material selection, construction management, operation and maintenance, as well as vegetation arrangement—a versatile and reusable evaluation framework is presented, tailored to facilitate the optimal design of green roofs across diverse climatic regions. The research scope is limited to the scenarios of existing building roof renovations, with a focus on comparing key indicators of green roofs and ordinary roofs. The aim is to provide scientific and quantifiable basis for urban planners and architects in making decisions on green building renovations, and to promote the large-scale application of green roof technology in urban sustainable development.

2. METHODS AND MATERIALS

The study adopts a systematic approach to evaluate the carbon benefits of rooftop garden design, namely green rooftop garden carbon balance accounting based on carbon balance. This method quantifies the CEs and absorption of rooftop gardens throughout their entire lifecycle to evaluate their contribution to urban thermal efficiency. The concept of building energy efficiency is integrated into the design of green roof gardens, finally constructing an evaluation index system. The framework diagram of the research technical route is shown in Figure 1.

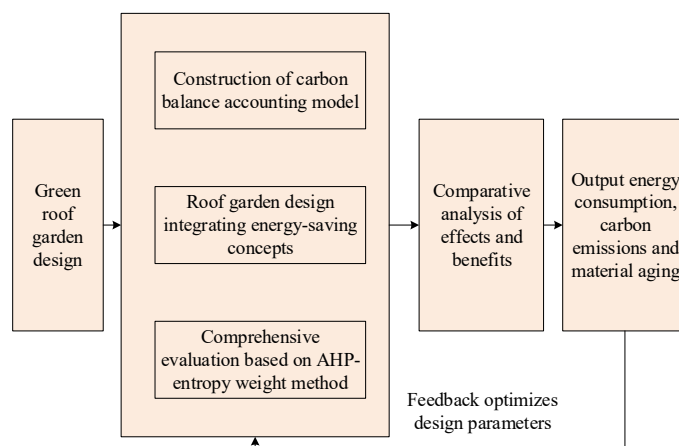


Fig. 1. Research the framework diagram of the technical route.

2.1 Carbon Balance Accounting for Green Roof Gardens based on Carbon Balance

The study systematically measures the carbon benefits of green roof garden design by constructing a carbon balance based evaluation framework. This framework evaluates the potential contribution of green roofs to improving urban thermal efficiency by quantifying their CEs and plant carbon absorption throughout their lifecycle. This method not only focuses on reducing CEs, but also on how green roofs can improve urban thermal environment and enhance urban thermal efficiency by lowering building surface temperature and reducing energy consumption. In the design of green

roof gardens, the research will explore the balance between CEs and plant carbon absorption throughout the entire lifecycle. This balance takes into account the energy and resource consumption caused by the production of hard materials during the construction process, as well as the resulting carbon dioxide emissions. In addition, the construction, maintenance, operation, and final demolition of gardens also involve energy consumption and CEs issues. In terms of carbon absorption, the carbon sequestration function of plants is the main pathway, playing a key role in maintaining the carbon balance of gardens [11], [12]. The carbon balance of rooftop gardens is shown in Figure 2.

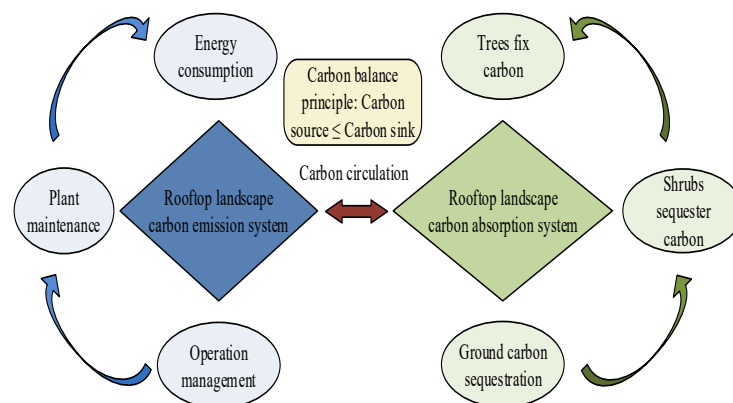


Fig. 2. Carbon balance diagram of roof garden.

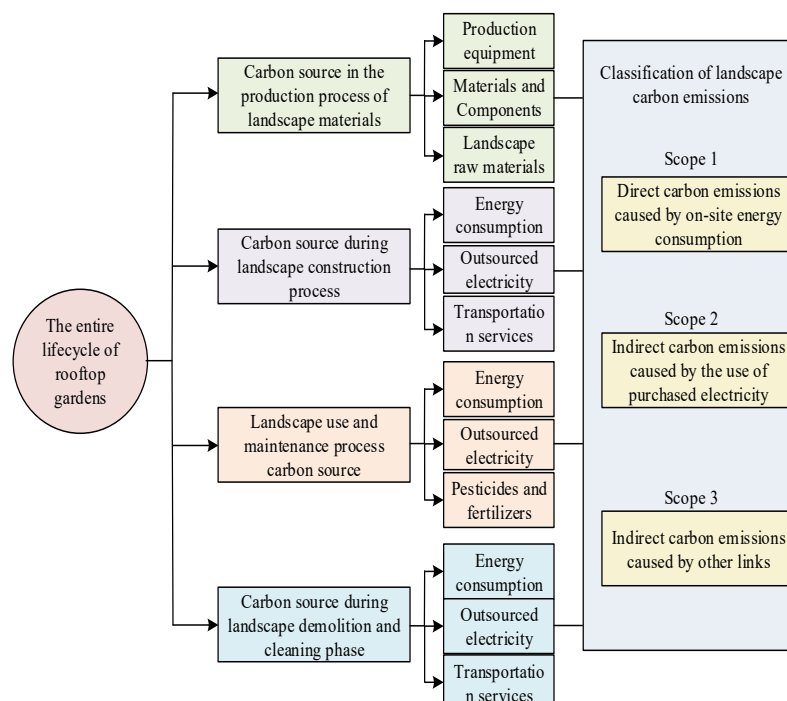


Fig. 3. CE accounting scope of roof garden design.

In Figure 2, reducing CEs and enhancing the carbon sequestration capacity of green spaces are key strategies for creating a low-carbon environment in rooftop landscaping. For rooftop garden design, the implementation of low-carbon should focus on achieving carbon neutrality. During the design and

construction process, efforts should be made to minimize activities that generate CEs and expand the coverage of green vegetation to enhance its carbon absorption capacity. Through precise quantitative assessment of CEs and carbon sinks, the goal is to achieve carbon neutrality by equating the CEs of rooftop

gardens with the carbon absorption of vegetation, known as the "zero carbon footprint" goal. With the continuous progress of ecological architecture, the evaluation system for the entire building cycle is relatively improved, forming a systematic evaluation process. The scope of CE accounting for rooftop garden design is shown in Figure 3.

In Figure 3, based on the division of the full cycle time stages, the calculation process and methods for each stage are sorted out. The primary task is to identify the main CE sources at each stage, and develop corresponding accounting standards based on the characteristics of these emission sources, ultimately constructing an accounting framework. To calculate the CEs of rooftop garden design throughout its entire lifecycle, based on the CE measurement standards of the construction industry, the lifecycle of rooftop garden design is divided into four stages: garden material preparation, garden construction, garden use and maintenance, and garden demolition and cleaning [13], [14]. The calculation of total CEs during the lifecycle is shown in Equation (1).

$$E_{LC} = E_{JC} + E_{SG} + E_{SY} + E_{GX} \quad (1)$$

In Equation (1), E_{LC} means the total CEs of the roof garden design throughout its entire lifecycle, the unit is kg CO₂-eq. E_{JC} represents the CEs generated during the preparation of garden materials, the unit is kg CO₂-eq. E_{SG} means the CEs during the construction phase of the garden, the unit is kg CO₂-eq. E_{SY} represents the CEs including the use and maintenance phase of the garden, the unit is kg CO₂-eq. E_{GX} means the CEs generated during the demolition and cleaning phase of the garden, the unit is kg CO₂-eq. In the CE analysis of rooftop garden design, material preparation, construction, and final demolition and cleaning stages are considered as one-time CE sources, which will not generate sustained CEs after the project is completed. The use and maintenance stages of gardens are considered periodic sources of CEs, which continue to generate CEs throughout the entire lifespan of the garden, usually calculated on an annual basis. The design of rooftop gardens mainly achieves carbon absorption through the carbon fixation effect of plants, which is continuous and calculated on an annual basis. By comparing the total CEs in rooftop garden design with the carbon sequestration of plants, it is possible to evaluate whether the carbon source and sink of the garden have reached a balance, as shown in Equation (2).

$$B = \frac{E_{LC}}{C_{LC}} \quad (2)$$

In Equation (2), B represents the carbon balance ratio. E_{LC} represents landscape CEs, the unit is kg CO₂-eq. C_{LC} represents plant carbon sequestration, the unit is kg CO₂-eq. If the value of B is equal to 1, it indicates that the rooftop garden design has achieved carbon

balance. The carbon balance model's emission factors preferentially adopted the "Building Carbon Emission Calculation Standard" GB/T 51366 of the 2022 edition and the "Power Grid, Road Transport, and Building Materials Manufacturing in South China Region" subset from the Ecoinvent 3.9 database. In case of data gaps, the measured samples of building materials manufacturing enterprises in Shenzhen from 2021 to 2023 were supplemented. The sample size was ≥ 30 groups. The red-edge vegetation index was verified through monthly unmanned aerial vehicle (UAV) remote sensing inversion from September 2022 to February 2024, with the deviation controlled within $\pm 5\%$. Uncertainty analysis was conducted using Monte Carlo simulation with 10,000 samples. The input parameters simultaneously took into account the normal distribution variations of emission factors, material usage, and vegetation yield. The results showed that the 90% confidence interval of the carbon balance ratio was 0.96-1.04, demonstrating the robustness and reliability of the model output.

2.2 Green Roof Landscape Design Incorporating Building Energy Efficiency Concepts

After constructing a carbon balance accounting model for rooftop gardens, research is conducted on incorporating building energy-saving concepts into the design of green rooftop gardens. The concept of building energy efficiency refers to a series of measures and technologies taken throughout the entire process of building design, construction, use, and maintenance to reduce energy consumption, improve energy utilization efficiency, and achieve the goal of saving resources, protecting the environment, and reducing operating costs. The implementation of energy-saving concepts in buildings can help reduce greenhouse gas emissions, combat global climate change, and save long-term energy costs for building owners and users, becoming an indispensable part of building design and construction. The case building selected was a scientific research office building located in the central area of Futian District, Shenzhen City, which was completed in June 2022. The building had 12 floors and its roof was accessible to people. The measured area of the roof was 1,860 square meters. The structural load was confirmed by a third-party test in July 2022 to meet the additional load requirements for the roof garden. The experimental observation was continuously carried out from September 1, 2022 to February 29, 2024, lasting for a full 18 months, covering two complete summer and winter cycles. During this period, no roof leakage or large-scale vegetation replacement occurred. All temperature, humidity, energy consumption and material aging data were collected and cross-verified on a monthly basis to ensure that the results corresponded to the typical humid and hot climate conditions in Shenzhen. To accurately calculate the building's energy consumption, the study placed the rooftop garden and the ordinary roof in two symmetrical areas on the north and south sides of the same scientific research office building, each covering an area of 930 square meters. From September 1, 2022, to February 29, 2024, the sub-

item metering system simultaneously collected the following loads over a period of 18 months: the electricity consumed by air conditioning units, fresh air handling units, and terminal fan coil units; the electricity consumed by roof lighting and landscape lamps; the electricity consumed by the automatic drip irrigation pump and solenoid valve in the rooftop garden; and the electricity consumed by the elevator machine room, pressurized water pump, and exhaust fan in the roof equipment room. All the data were recorded at 15-minute intervals. The cumulative volume was exported monthly and abnormal peaks were excluded. The final conversion was $\text{kWh/m}^2\cdot\text{a}$ to ensure that the energy consumption comparison only reflects the changes in air conditioning and equipment loads caused by the thermal differences of the roof. 16 temperature sensing devices were installed in the experimental area to record temperature changes in the covered and uncovered roof areas, in order to evaluate the impact of vegetation on roof temperature regulation, including cooling and insulation effects. The experimental area was located in the central district of Futian District, Shenzhen City, in the hot summer and cold winter climate zone. Its geographical coordinates were $22^{\circ}32'$ north latitude and $114^{\circ}03'$ east longitude, with an altitude of approximately 18 meters. The third-party structural load test in July 2022 confirmed that it could meet the additional load requirements of the roof garden. The average annual total solar radiation in this area was $4.8 \text{ kWh m}^{-2} \text{ d}^{-1}$. The average annual temperature was 23.0°C . The extreme maximum temperature in July was 38.9°C , and the extreme minimum temperature in January was 6.4°C . The average annual relative humidity was 78%. The annual precipitation was 1925 mm. The precipitation from May to September accounted for 74%

of the annual total. The average annual wind speed was 2.4 m s^{-1} . The prevailing wind direction was southeast. The vegetation layer of the green roof selects four perennial drought-tolerant succulent plants, namely *Fuldaglut*, *Weihenstephaner Gold*, *Sedum polytrichoides* and *Sedum sarmentosum*. The mixed seeding ratio was 3:3:2:2, the designed height of the canopy was 12-15 cm, and the green period throughout the year was ≥ 300 days. The substrate layer was a 10 cm thick lightweight mineral substrate. The model of the 16 temperature sensors was uniformly Pt100 RTD (IEC 60751 Class A, $\pm 0.15^{\circ}\text{C}$), the probe diameter was 6 mm, the length was 50 mm, and the response time $\tau_{0.5} < 4 \text{ s}$. All sensors were calibrated in a CNAS-certified Fluke 7341 constant temperature water bath ($\pm 0.01^{\circ}\text{C}$) at two points of 20°C and 40°C , with a calibration coefficient $R^2 > 0.999$. A comparison was made again before on-site installation to ensure that the deviation was $< 0.05^{\circ}\text{C}$. The sensor deployment positions included 8 at the matrix-air interface beneath the vegetation, 4 on the exposed control roof surface, and 4 on the lower surface of the indoor ceiling. The collection interval was 5 minutes. The data were transmitted in real time to the local edge computing gateway through the LoRa wireless module and simultaneously backed up in the cloud. The diversity of vegetation configuration has a significant impact on indoor temperature and is equally critical to building energy efficiency performance. It is particularly important to determine the main factors and ideal conditions that affect energy-saving effects before carrying out roof greening planning [15], [16]. The building faces north and south without any neighboring buildings blocking it, with excellent ventilation and lighting conditions. The specific standards for different types of roof loads are shown in Table 1.

Table 1. Standard values of different types of roof loads and their correlation coefficients.

| Serial number | Roof type | Standard load value (kN/m^2) | Combination coefficient | Frequency factor | Quasi-permanent value coefficient |
|---------------|------------------------|---|-------------------------|------------------|-----------------------------------|
| 1 | Non-human movable roof | 0.5 | 0.7 | 0.5 | 0.0 |
| 2 | Movable roof | 2.0 | 0.7 | 0.5 | 0.4 |
| 3 | Green roof area | 3.0 | 0.7 | 0.6 | 0.5 |
| 4 | Rooftop sports arena | 4.5 | 0.7 | 0.6 | 0.4 |

In Table 1, the standard load value for non-personnel activity roofs is 0.5 kN/m^2 , with a combination coefficient of 0.7, a frequency coefficient of 0.5, and a quasi-permanent value coefficient of 0.0. The standard load value for personnel activity roof is 2.0 kN/m^2 , with a combination coefficient of 0.7, a frequency coefficient of 0.5, and a quasi-permanent value coefficient of 0.4. The standard load value for the rooftop green area is 3.0 kN/m^2 , with a combination coefficient of 0.7, a frequency coefficient of 0.6, and a quasi-permanent coefficient of 0.5. The standard load value for the rooftop sports field is 4.5 kN/m^2 , with a combination coefficient of 0.7, a frequency coefficient of 0.6, and a quasi-permanent coefficient of 0.4. These data provide load reference standards for roof design and their variation coefficients under different usage conditions. According to the *General Code for Engineering*

Structures (GB 55001-2021), the roof design bearing capacity of the building is 3 kN/m^2 . If the weight of decorative elements is added, the bearing capacity should reach 3.5 kN/m^2 or more. The specific configuration of roof greening parameters is shown in Table 2.

In Table 2, the vegetation height was set to 12 centimeters, the radiation capacity of the leaves was 95%, the reflection capacity of the leaves was 22%, and the leaf area index reached 1. The minimum resistance value of stomata was set at 150 seconds per meter, the soil surface roughness was at a moderate level, and the soil layer thickness was 10 centimeters. The thermal conductivity of dry soil was 0.35 watts per meter per Kelvin, its density was 1184 kilograms per cubic meter, and its specific heat capacity was 0.81 joules per kilogram per Kelvin. To truly integrate the "concept of

building energy conservation" into the roof garden design, a double-layer composite insulation system of 50mm thick vacuum insulation board and 30mm thick phase change gypsum board was added below the vegetation layer. Continuous aluminum foil reflective film was arranged on the inner side of the parapet wall on the roof, with a reflectivity of 0.9, to reduce the heat gain from long-wave radiation. The HVAC side adopted a variable refrigerant flow multi-split system. The rated

refrigeration performance coefficient of the main unit was 5.6 and the heating performance coefficient was 4.8. The indoor terminal used DC brushless fan coil units and was equipped with CO₂ concentration sensors. The total heat recovery efficiency of the fresh air unit's rotor was $\geq 75\%$. The irrigation system was supplied by a 5 m³ stainless steel rainwater tank on the roof and municipal water replenishment through dual channels, and the water pump operates at variable frequency.

Table 2. Setting of roof greening parameters.

| Roof greening parameter | Units | Set value |
|--|-------------------|--------------|
| Plant height | m | 0.12 |
| Leaf area index | / | 1 |
| Leaf reflectance | / | 0.22 |
| Blade emissivity | / | 0.95 |
| Minimum stomatal resistance | s/m | 150 |
| Soil roughness | / | Medium rough |
| Soil thickness | m | 0.1 |
| Thermal conductivity of dry soil layer | W/m·k | 0.35 |
| Dry soil density | kg/m ³ | 1184 |
| Specific heat capacity of dry soil | J/kg·K | 0.81 |
| Solar radiation absorption rate of dry soil | / | 0.7 |
| Visible light absorption rate of dry soil | / | 0.7 |
| Dry soil saturated volume moisture content | / | 0.5 |
| Residual volume moisture content of dry soil | / | 0.01 |
| Initial volume moisture content of dry soil | / | 0.1 |
| Water diffusion calculation method | / | Advanced |

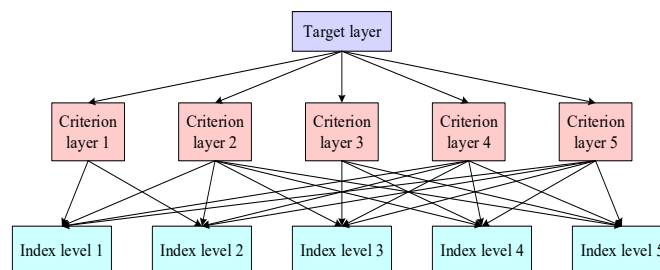


Fig. 4. Evaluation architecture based on AHP.

2.3 Green Roof Landscape Evaluation based on AHP - Entropy Weight Method

After designing a green roof garden, research focuses on building a low-carbon evaluation framework for roof garden design with carbon balance as the core concept. When constructing the AHP evaluation system, the study adopted a targeted invitation approach from October to December 2023, gathering a total of 21 experts with over ten years of professional or research experience in the fields of green buildings, urban thermal environment, and sustainable landscapes to participate in the scoring. Among them, there were 9 university professors, 6 green building consulting engineers from design institutes, 4 technical committee members from government construction administrative departments and industry associations, and 2 technical directors of real estate development with international

LEED AP qualifications. All experts independently filled out the pre-tested paper questionnaires. Pairwise comparisons were made between the criterion layer and the index layer using the 1-9 scale method. A total of 21 valid questionnaires were retrieved, and the consistency ratio CR values were all less than 0.1, meeting the acceptable consistency requirements recommended by Saaty. To reduce subjective bias, the study cross-validated the expert judgment matrix with the on-site measured data of Shenzhen from 2022 to 2024, GB/T 50378-2019 "Green Building Evaluation Standard", and the IPCC 2021 emission factor database. The weight uncertainty was quantified through Monte Carlo simulation (10,000 samples). The results showed that the width of the 90% confidence interval of each index weight did not exceed ± 0.02 , indicating that the evaluation system had good robustness [17], [18]. The

evaluation system architecture based on AHP is shown in Figure 4.

In Figure 4, the evaluation system architecture based on AHP includes the objective layer, criterion layer, and indicator layer. After establishing the hierarchical structure model, the study uses a scoring method from 1 to 9 to compare each evaluation factor in pairs to form a judgment matrix. When making pairwise comparisons, the number 1 suggests that both factors hold equal significance, the number 3 suggests that one factor carries somewhat greater weight, the number 5 suggests that one factor holds considerable importance, the number 7 suggests that one factor is of utmost importance, and the number 9 suggests that one factor is of utmost importance. The numbers 2, 4, 6, and 8 are the middle values of the above values. Based on these criteria, the research analyzes and compares the scores of experts, and constructs a judgment matrix [19], [20]. Based on the constructed judgment matrix, the

maximum eigenvalue is calculated and the corresponding eigenvector is derived accordingly. After normalization, the numerical values obtained from these feature vectors are the relative importance ranking weights of each level factor relative to higher-level factors. In the evaluation system of rooftop garden design, the AHP is used to determine weights. Although the rationality of its results is usually considered high, it inevitably carries subjectivity. The entropy weight rule is an objective weight allocation method based on data information mining, which does not rely on the subjective opinions of experts and decision-makers, but may deviate from the actual situation as a result [21], [22]. The integration of these two methods served to mitigate the subjective bias inherent in the AHP and made up for the deficiency of subjective judgment in the Entropy Weight Method. The evaluation index system for green roof gardens based on AHP - Entropy Weight Method is shown in Figure 5.

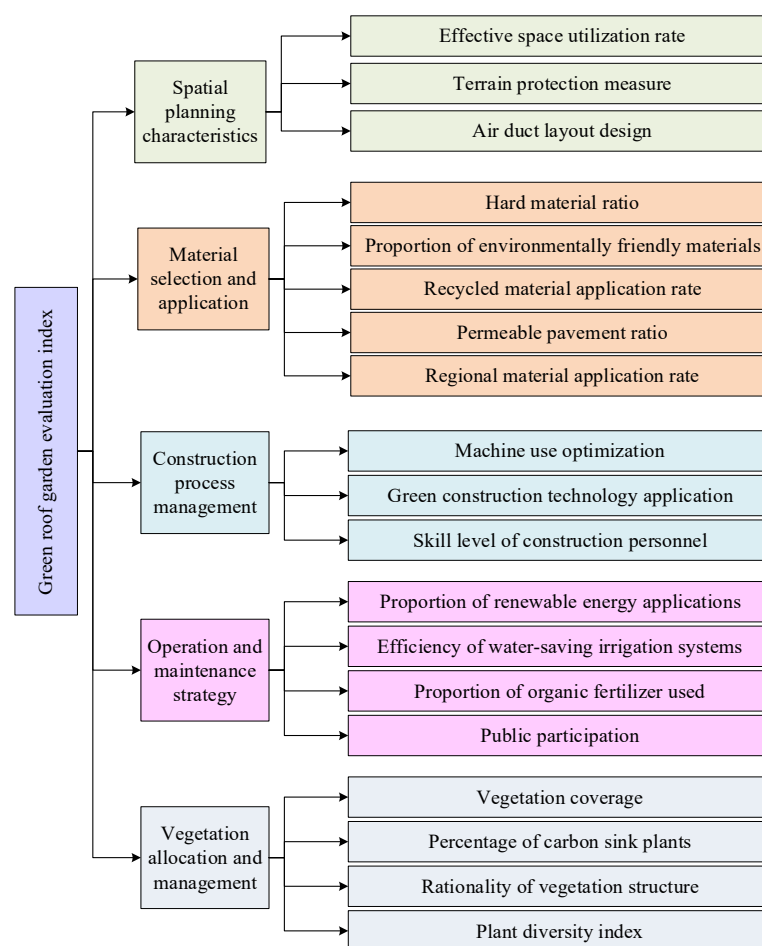


Fig. 5. Green roof garden evaluation index system.

In Figure 5, the evaluation index system for green roof gardens includes multiple levels. In terms of spatial planning characteristics, the evaluation indicators are further refined into effective space utilization rate, terrain protection measures, and air duct layout design. In terms of material selection and application, it involves the proportion of hard materials, the proportion of environmentally friendly materials, the application rate of recycled materials, the proportion of permeable

pavement, and the application rate of regional materials. Construction process management includes optimizing the use of machinery, applying green construction techniques, and assessing the skill level of construction personnel. The evaluation indicators for operation and maintenance strategies include the proportion of renewable energy applications, the efficiency of water-saving irrigation systems, the proportion of organic fertilizer use, and public participation. The evaluation

indicators for vegetation configuration and management include vegetation coverage, proportion of carbon sink plants, rationality of vegetation structure, and plant diversity index.

3. RESULTS

Firstly, the AHP - Entropy Weight Method was applied to allocate weights to the evaluation index system of green roof gardens, in order to determine the importance of each evaluation index. In addition, a comparative analysis was conducted on the differences in energy

consumption, CEs, and aging rate of building surface materials between green roofs and common building roofs, revealing the advantages of green roofs in energy conservation, consumption reduction, and prolonging material service life.

3.1 Evaluation Results of Green Roof Landscape Based on AHP - Entropy Weight Method

The weights of the green roof garden index evaluation system based on AHP - Entropy Weight Method are in Table 3.

Table 3. Weight of green roof garden index evaluation system.

| Primary index | Secondary index | Three-level index | Weights |
|------------------------------------|--------------------------------------|--|---------|
| Green roof garden evaluation index | Spatial planning characteristics | Effective space utilization rate | 0.0252 |
| | | Terrain protection measure | 0.0704 |
| | | Air duct layout design | 0.0372 |
| | Material selection and application | Hard material ratio | 0.0158 |
| | | Proportion of environmentally friendly materials | 0.0456 |
| | | Recycled material application rate | 0.0851 |
| | | Permeable pavement ratio | 0.0294 |
| | | Regional material application rate | 0.0038 |
| | | Machine use optimization | 0.0151 |
| | | Green construction technology application | 0.0558 |
| | Construction process management | Skill level of construction personnel | 0.0991 |
| | | Proportion of renewable energy applications | 0.1278 |
| | | Efficiency of water-saving irrigation systems | 0.0156 |
| | | Proportion of organic fertilizer used | 0.0754 |
| | Operation and maintenance strategy | Public participation | 0.1052 |
| | | Vegetation coverage | 0.0411 |
| | | Percentage of carbon sink plants | 0.0354 |
| | | Rationality of vegetation structure | 0.0216 |
| | | Plant diversity index | 0.0954 |
| | Vegetation allocation and management | | |
| | | | |
| | | | |
| | | | |
| | | | |

In Table 3, the weight of effective space utilization rate in spatial planning characteristics was 0.0252, terrain protection measures were 0.0704, and air duct layout design was 0.0372, indicating that the importance of air duct layout design in spatial planning was slightly higher than the other two indicators. In terms of vegetation configuration and management, the weight of vegetation coverage was 0.0411, the proportion of carbon sink plants was 0.0354, the rationality of vegetation structure was 0.0216, and the plant diversity index was 0.0954. The weight of vegetation coverage was the highest, indicating the importance placed on coverage in vegetation management. According to the evaluation system of green roof garden indicators, the green roof designed in the research was evaluated. The evaluation results of green roof garden indicators are shown in Table 4.

In Table 4, in terms of spatial planning characteristics, the effective space utilization rate score was 85, the terrain protection measures score was

slightly lower at 80, and the air duct layout design score was the highest at 88, indicating that the performance of air duct layout design was the most outstanding in spatial planning. Overall, the evaluation index system for green roof gardens showed the performance of each evaluation dimension. Among them, the air duct layout design, proportion of environmentally friendly materials, application of green construction technology, and vegetation coverage rate performed the best, while the application rate of recycled materials, proportion of organic fertilizers, and plant diversity index scored relatively low, indicating that these aspects needed more attention and improvement.

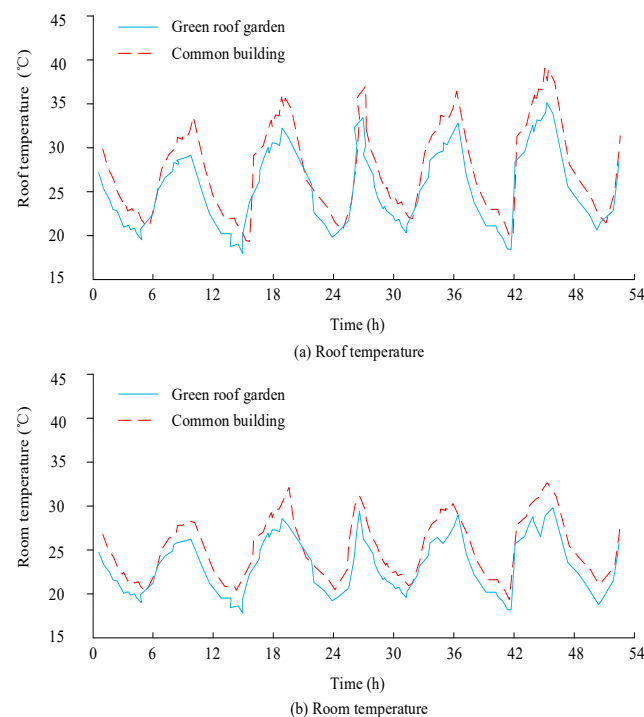
3.2 Analysis of Green Roof Landscape Effect

Comparing the green roof garden designed for research with common buildings, the temperature changes of the green roof garden and common building roofs in summer are shown in Figure 6.

Table 4. Green roof garden index evaluation results

| Primary index | Secondary index | Three-level index | Score |
|------------------------------------|--------------------------------------|--|-------|
| Green roof garden evaluation index | Spatial planning characteristics | Effective space utilization rate | 85.3 |
| | | Terrain protection measure | 80.1 |
| | | Air duct layout design | 88.4 |
| | Material selection and application | Hard material ratio | 75.0 |
| | | Proportion of environmentally friendly materials | 90.2 |
| | | Recycled material application rate | 70.4 |
| | | Permeable pavement ratio | 82.7 |
| | | Regional material application rate | 78.5 |
| | Construction process management | Machine use optimization | 85.0 |
| | | Green construction technology application | 92.3 |
| | | Skill level of construction personnel | 80.7 |
| | Operation and maintenance strategy | Proportion of renewable energy applications | 88.1 |
| | | Efficiency of water-saving irrigation systems | 84.5 |
| | | Proportion of organic fertilizer used | 76.2 |
| | Vegetation allocation and management | Public participation | 81.6 |
| | | Vegetation coverage | 90.0 |
| | | Percentage of carbon sink plants | 87.4 |
| | | Rationality of vegetation structure | 83.2 |
| | | Plant diversity index | 75.3 |

Note: The score was obtained by truncating the average of the 9-level continuous scale scores of 21 experts, excluding the extreme 2.5%, and then multiplying it by 100, with one decimal place retained.

**Fig. 6. Green garden and common building roof house summer temperature variation.**

In Figure 6 (a), the coverage of vegetation on the roof could significantly reduce the daily temperature difference of the roof, with a maximum temperature difference of about 4.8 °C. Compared to the traditional concrete roof with a temperature difference of 10.2 °C, the vegetation covered roof exhibited milder temperature fluctuations. This means that roofs covered with vegetation were more effective in temperature regulation, reducing extreme temperature changes,

which was beneficial for the durability and maintenance of buildings. In Figure 6 (b), the effect of roof greening on reducing indoor environmental temperature cannot be ignored, as this technology could lead to a 4 °C decrease in indoor temperature. This had a positive impact on improving indoor comfort and reducing air conditioning usage, thereby reducing energy consumption and CEs. The aging rate and service life of building surface materials are shown in Figure 7.

In Figure 7 (a), the roof building material of the green roof garden showed a slower aging rate, with a degree of aging of only 39% after 30 months. In contrast, the aging rate of roof building materials in common buildings was faster, reaching 78% after 30 months. In Figure 7 (b), the remaining life of the building surface materials for green garden roofs was significantly higher than that of common buildings, indicating the significant advantage of roof greening in extending the service life of materials.

3.3 Analysis of Carbon Balance and Urban Thermal Efficiency Benefits

The CEs of green garden roofs and common building roofs are shown in Figure 8. The total CEs calculation scope for the entire life cycle comprehensively covered four stages: material preparation (including the

production and transportation of raw materials such as substrates, plants, and structural layers), construction and building (including mechanical use and labor energy consumption), operation and maintenance (including annual periodic emissions such as irrigation, fertilization, and pruning), and demolition and cleaning (including waste transportation and treatment). The new note in the text pointed out that among the 3 tons of CEs from green roofs, the material preparation stage accounted for approximately 42%, the construction stage about 15%, the cumulative 30 years of operation and maintenance about 38%, and the demolition stage about 5%. Among the 5 tons of CEs from a regular roof, the material preparation stage accounted for as high as 55%, the operation and maintenance stage accumulated to 35% due to the lack of vegetation carbon sink offsetting, and the remaining stages accounted for 10%.

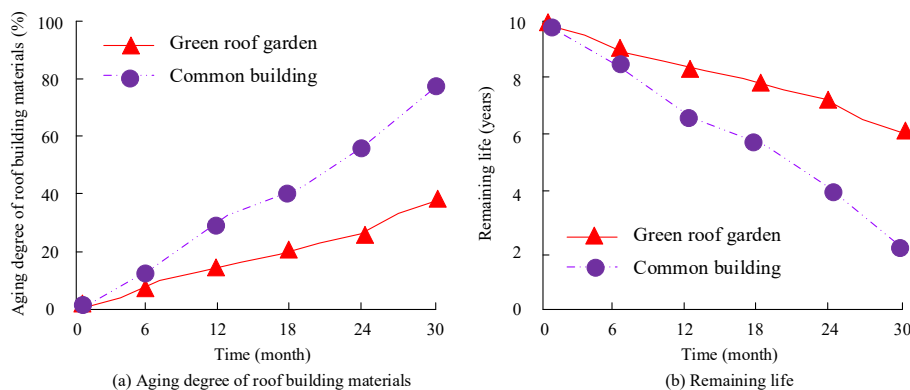


Fig. 7. Aging rate and service life of building surface materials.

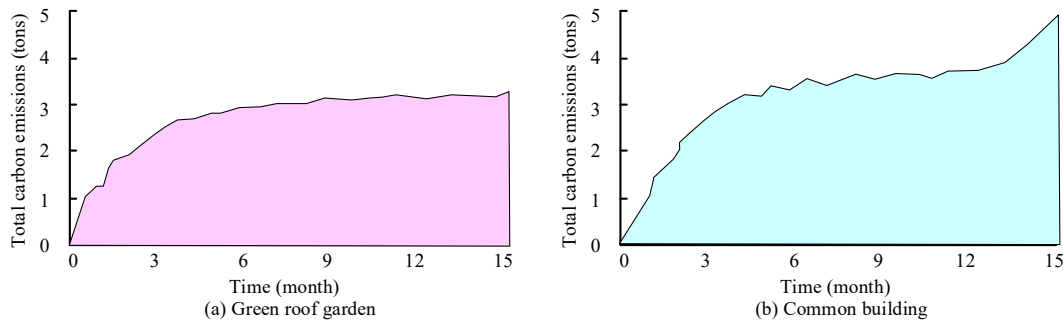


Fig. 8. CE of green garden roof and common building roof.

In Figure 8 (a), the CEs from the green garden roof were 3 tons. This indicated that green garden roofs had a positive effect on reducing CEs, with lower CEs compared to common building roofs. Green vegetation absorbs carbon dioxide through photosynthesis, which helps reduce the carbon content in the atmosphere and thus lower the overall carbon footprint of buildings. In Figure 8 (b), the CEs of common building roofs were 5 tons, which was higher than those of green garden roofs. Common building roofs lack vegetation coverage and cannot effectively absorb carbon dioxide through

photosynthesis, resulting in relatively high CEs. The thermal efficiency benefits of green garden roofs and common building roofs are shown in Figure 9. The annual energy cost was obtained by multiplying the average time-of-use electricity price in Shenzhen from 2022 to 2024 by the measured annual electricity consumption. The difference in cumulative electricity charges for the two types of roofs over a 30-year life cycle was discounted at an 8% social discount rate, and then divided by the initial investment in the green roof increment to obtain the economic benefit ratio.

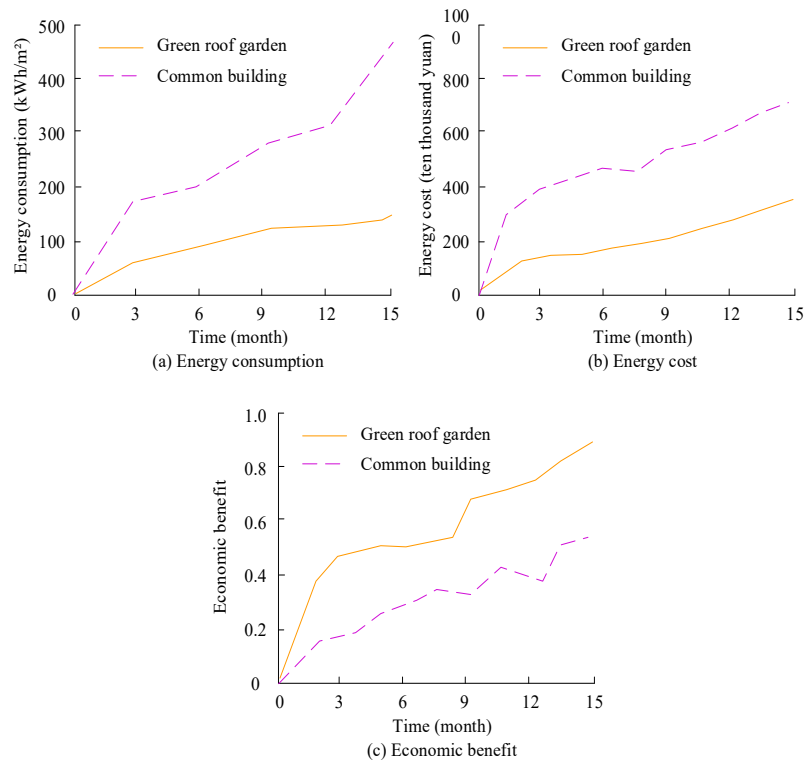


Fig. 9. Thermal efficiency benefits of green garden roofs and common building roofs.

In Figure 9 (a), the annual energy consumption of green garden roofs was 180 kWh/m², while the annual energy consumption of common building roofs was 490 kWh/m². Green garden roofs have significant advantages in energy conservation, with much lower energy consumption than common building roofs. In Figure 9 (b), the annual energy cost of green garden roofs was 2 million yuan, which is lower than the energy cost of common building roofs, which was 7.5 million yuan. Overall, green garden roofs had better thermal efficiency benefits. In Figure 9 (c), the economic benefits of green garden roofs exceeded 0.9, which further confirmed the superiority of green garden roofs in terms of economic benefits.

To further explain the role path of roof vegetation in reducing energy consumption and delaying material aging, the research conducted a mechanism analysis based on measured data and microscopic material detection. In terms of thermal efficiency, the measured data at the vegetation-matrix-air interface showed that during the day, the canopy took away sensible heat through transpiration, and the surface temperature of the substrate was 8.3°C lower than that of the exposed roof. The long-wave radiation shielding effect of the vegetation canopy at night made the surface temperature 2.1°C higher than that of the exposed roof. The reduction in daily temperature difference directly lowered the number of thermal stress cycles in the roof structural layer by approximately 46%, thereby reducing the air conditioning load on the top floor by 27%. The coupled simulation of infrared thermal imaging and CFD further indicated that the sedum patches arranged in a "triangular" shape could induce a wall adhesion turbulence of 0.15 m s⁻¹ at an ambient wind speed of 0.5 m s⁻¹, significantly enhancing the convective heat transfer coefficient between the roof and the air to 12.8

W m⁻² K⁻¹ and reducing the heat transfer to the lower insulation layer. In terms of material aging, a 30-month accelerated aging experiment combined with SEM-EDX analysis revealed that vegetation shading reduced the cumulative ultraviolet irradiation on the surface of roof sheets by 51%, and the peak surface temperature dropped by 11 °C. Correspondingly, the growth rate of the carbonyl index (C=O) of SBS modified asphalt rolls decreased from 0.18 month⁻¹ in the exposed group to 0.07 month⁻¹ in the green group, and the surface cracking density decreased from 2.4 mm mm⁻² to 0.9 mm mm⁻². In addition, the vegetation's retention of precipitation reduced the dry-wet cycle range of the rolls, inhibited the expansion of micro-cracks caused by freeze-thaw cycles, and comprehensively delayed the attenuation of the ultimate tensile strength of the rolls by approximately 42%, thereby extending the expected service life from the conventional 15 years to over 25 years.

4. CONCLUSION

To explore the capability of green roof garden design incorporating building energy-saving concepts in urban thermal efficiency benefits, and analyze its impact on the aging of building surface materials, a carbon balance accounting model for roof gardens based on carbon balance was constructed. The energy consumption, CEs, and material aging rate of green roofs and common building roofs were compared and analyzed. The research results indicated that the coverage of rooftop vegetation could significantly reduce the daily temperature difference of the roof, with a maximum temperature difference of about 4.8°C, while the temperature difference of traditional concrete roofs reached 10.2°C. The annual energy consumption of

green roofs was 180 kWh/m², with a CE of 3 tons and a material aging degree of 39%, all lower than common buildings. Green garden roofs not only had a positive effect on reducing energy consumption and CEs, but also demonstrated significant advantages in reducing energy costs and improving economic benefits. These advantages make green garden roofs an important measure to promote building energy efficiency and sustainable development, promote the stability and durability of building structures, and thus extend the service life of buildings. The CE analysis framework constructed by the research can be directly embedded into the urban planning management platform and the green building pre-assessment system, helping decision-makers quickly identify high-carbon links during the scheme comparison stage and optimize material selection and vegetation configuration. Local governments should be provided with differentiated technical and economic parameters when they formulate policies for roof greening subsidies and carbon reduction incentives. However, the research experimental samples were limited to a south-facing, unobstructed middle-level office building in a hot summer and cold winter area. The on-site measured data of the carbon balance calculation during the demolition stage were missing. It was only estimated based on the regional statistical average value, which may underestimate the CEs generated by the actual demolition transportation and waste treatment. The weights of key indicators such as public participation and water-saving irrigation efficiency in the evaluation index system were comprehensively determined by the AHP-entropy weight method. Affected by the number of expert samples and regional experience differences, subjective biases have not been completely eliminated. Future research needs to further expand the sample size and deepen model application, to provide more comprehensive decision support for the promotion and application of green roofs.

DECLARATIONS

Author Contributions: R.G. writing—original draft preparation and data curation, S.Z. investigation and investigation and writing—review and editing.

Data Availability: The data supporting the findings of this study are available within the article.

Conflicts of Interest: The authors declare no conflict of interest.

Funding: No funding was received.

REFERENCES

- [1] Law C.M.Y., Hui L.C., Jim C.Y. and Ma T.L., 2021. Tree species composition, growing space and management in Hong Kong's commercial sky gardens. *Urban Forestry and Urban Greening* 64(4): 127267.1-127267.11.
- [2] Maltseva I.N., Shvalev D.M. and Tkachuk K.A., 2021. Problems and solutions for green roofs. *IOP Conference Series: Materials Science and Engineering* 1066(1): 12012-12021.
- [3] Saracoglu O.A., Cakar H., Akat H., and Adanacioglu H., 2022. Performance analysis of different geotextile materials in extensive roof garden designs. *Journal of Environmental Engineering and Landscape Management: International Research towards Sustainability* 30(4): 484-492.
- [4] Usman A.M. and M.K. Abdullah. 2023. An assessment of building energy consumption characteristics using analytical energy and carbon footprint assessment model. *Green and Low-Carbon Economy* 1(1): 28-40.
- [5] Jamei E., Thirunavukkarasu G., Chau H.W., Seyedmahmoudian M, Stojcevski A., and Mekhilef S. 2023. Investigating the cooling effect of a green roof in Melbourne. *Building and Environment* 246(12): 1.1-1.21.
- [6] Rabbani M. and F. Kazemi. 2022. Water need and water use efficiency of two plant species in soil-containing and soilless substrates under green roof conditions. *Journal of Environmental Management* 302(Pt A): 113950-113967.
- [7] Liu J., Liu P., Wang X., Liu S., Wang G., and Shuang W.U., 2021. Design and construction of sponge city facilities in Changzhen depot of Shenzhen metro. *Journal of Shenzhen University Science and Engineering* 38(1): 20-26.
- [8] Akar H., Saracoglu O.A., Akat H., Kl C. and Adanacolu H., 2023. The potential for using different substrates in green roofs. *Journal of Environmental Engineering and Landscape Management* 31(1): 44-51.
- [9] Gohari A., Gohari A., and Ahmad A. B., 2023. Importance of green roof criteria for residential and governmental buildings: A multi-criteria decision analysis. *Environmental Science and Pollution Research* 30(2), 3707-3725.
- [10] Durdyyev S., Koc K., Karaca F., and Gurgun A.P., 2023. Strategies for implementation of green roofs in developing countries. *Engineering, Construction and Architectural Management* 30(6), 2481-2502.
- [11] Bortolini L. and V. Brasola. 2022. Simulating the impact of nature-based solutions on runoff control by using i-Tree Hydro: a case study in Padua (Italy). *Acta Horticulturae* 1345(47): 351-358.
- [12] Semeraro T., Scarano A., Buccolieri R., Santino A., and Aarrevaara E., 2021. Planning of urban green spaces: An ecological perspective on human benefits. *Land* 10(2): 1-26.
- [13] Reichelstein S., 2024. Corporate carbon accounting: balance sheets and flow statements. *Review of Accounting Studies* 29(3): 2125-2156.
- [14] Piatka D.R., Frank A.H., and Koehler I., 2022. Balance of carbon species combined with stable isotope ratios show critical switch towards bicarbonate uptake during cyanobacteria blooms. *Science of the Total Environment* 803(3): 1-13.
- [15] Pamponet M.C., Maranduba H.L., Neto J.A.A., and Rodrigues L.B., 2022. Energy balance and carbon footprint of very large-scale photovoltaic power plant. *International Journal of Energy Research* 46(5): 6901-6918.

- [16] Lai Q., Zheng H., Tang Z., Bi D., Chen N., and Liu, X., 2021. Balance of N-doping engineering and carbon chemistry to expose edge graphitic N sites for enhanced oxygen reduction electrocatalysis. *ACS Applied Materials and Interfaces* 51(13): 61129-61138.
- [17] Li X., Wang Y., Wu K., and Feng Z., 2023. Analysis and prediction of carbon balance in production-living-ecological space of Henan Province, China. *Environmental Science and Pollution Research* 30(30): 75973-75988.
- [18] Ran L., Wang X., Li S., Zhou Y., Xu Y. Chan C.N., Fang N., Xin Z., and Shen H., 2022. Integrating aquatic and terrestrial carbon fluxes to assess the net landscape carbon balance of a highly erodible semiarid catchment. *Journal of Geophysical Research Biogeosciences* 127(3): 1-15.
- [19] Yu Z., Liu Z., Chen M., Zhao J., Hao C., Zhang Y., and Li X., 2023. Optimizing charge balance in carbon dot-based LEDs for enhanced performance. *Journal of Materials Chemistry C* 11(46): 16280-16287.
- [20] Yuan Z., Zhen Y., Juan Z., and Wenjie Z., 2023. Study on the initial carbon quota allocation and spatial balance compensation strategy at the provincial level in China. *Environmental Science and Pollution Research* 30(25): 67150-67171.
- [21] Ester G.D.A., Gazol A., and Ignacio Querejeta J., 2022. The role of nutritional impairment in carbon-water balance of silver fir drought-induced dieback. *Global Change Biology* 28(14): 4439-4458.
- [22] Ejarque E., Scholz K., Wohlfahrt G., Battin T.J., Kainz M.J., and Schelker J., 2021. Hydrology controls the carbon mass balance of a mountain lake in the eastern European Alps. *Limnology and Oceanography* 66(6): 2110-2125.

